2-DOF Camera Stabilization Platform for Robotic Fish Based on Active Disturbance Rejection Control*

Pengfei Zhang, Zhengxing Wu, Jian Wang, Min Tan and Junzhi Yu, *Senior Member, IEEE*

***Abstract*— This paper proposes a novel 2-DOF stabilization platform for vision application of robotic fish to enhance the stability of image and reject the periodic disturbance from yaw and roll channels caused by fish's swimming. The problem formulation and system framework of camera stabilization are first discussed. In order to achieve better control effect, forward and inverse kinematics of the 2-DOF gimbal are derived, which combine the feedback of IMU and target states to calculate controllers' ideal input. Meanwhile, linear active disturbance rejection control (ADRC) without tracking differentiator is adopted in our system, on account of its superior performance to compensate uncertainties and disturbance. Finally, experimental results demonstrate that the error angle of ADRC is obviously smaller than PD and feedback-feedforward control. Furthermore, compared with 1-DOF stabilization platform, the 2-DOF one exhibits the overwhelming advantage about the enhancement of image stability.**

I. Introduction

Since the first robotic tuna was designed by MIT in 1995 [1], fish robot imitating the locomotion of natural fish is developing into an attractive research area. Due to the high maneuverability and low-disturbance, robotic fish is more appropriate than autonomous underwater vehicle (AUV) for several tasks, such as underwater monitoring, searching, exploration and rescue. In early stage, enhancing the maneuverability of robotic fish is the major research emphasis. Liu *et al.* designed a multijoint fish 'G9' and proposed an approach to model carangiform fish-like swimming motion [2]. Imitating the appearance of tuna, BIOSwimmer whose tail was equipped with a propeller was developed, which reached maximum speed over 5 knots [3]. Yu *et al.* proposed an active turn control method for a multilink dolphin robot, on which frontflip and backflip maneuvers were first implemented [4]. Su *et al.* replicated fast C-start maneuvers on a multijoint fish. It could achieve a peak turning speed of approximately 670°/s [5]. Wu *et al.* developed an esox lucius robotic fish and implemented three-dimensional (3D) high maneuvers [6]. Besides superior maneuverability, well environmental perception ability is also extremely essential for improving the applicability and practicability of robotic fish. Compared with sonar and other sensors, camera possesses the advantages of abundant information, mature algorithms, low cost and compact size. In [7], 3-D positioning based on an artificial landmark and embedded vision-based tracking control for robotic fish was investigated. Wang *et al.* proposed an online high-precision probabilistic localization method, which combined the informations from the onboard camera and low-cost inertial measurement unit (IMU) [8]. Visual perception ability provides more novel solutions for some problems associated with robotic fish. However, camera shaking caused by rhythmic oscillations of posterior body and caudal fin is a challenging issue, which severely depresses the visual application in robotic fish.

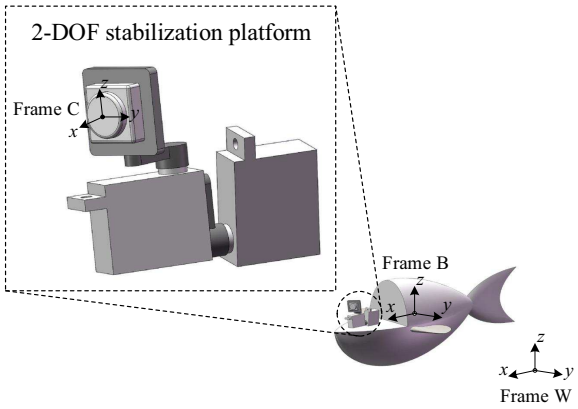

Fig. 1. The schematic diagram of 2-DOF stabilization platform for robotic fish.

The similar problem also appears in other robot domain. Aiming to stabilize the head of humanoid robot SABIAN during walking, Falotico *et al.* designed an adaptive model based on feedback error learning (FEL) and applied neural network to compute head inverse kinematics [9]. Inspired by binocular vestibule-ocular reflex, a bionic eye using a three degree of freedom (DOF) spherical parallel mechanism (SPM) was proposed to overcome vision instability [10]. Hurák *et al.* developed an inertially stabilized double gimbal system equipped on unmanned aerial vehicle (UAV), and proposed the control schemes for stabilization and pointing&tracking task [11]. A reactive 3-DOF camera stabilized system was designed for rescue robot, which supported camera through ball bears and adopted orientation control mechanism inspired by satellite control [12]. Although these solutions achieve remarkable results in their own application, they are not suitable for robotic fish owing to large volume

*This work was supported by the National Natural Science Foundation of China (nos. 61725305, 61633004, and 61633017).

P. Zhang, Z. Wu, J. Wang and M. Tan are with the State Key Laboratory of Management and Control for Complex Systems, Institute of Automation, Chinese Academy of Sciences, Beijing 100190, China and University of Chinese Academy of Sciences, Beijing 100049, China (e-mail: zhangpengfei2017@ia.ac.cn, zhengxing.wu@ia.ac.cn, wangjian2016@ia.ac.cn, min.tan@ia.ac.cn).

J. Yu is with the State Key Laboratory of Management and Control for Complex Systems, Institute of Automation, Chinese Academy of Sciences, Beijing 100190, China and the Beijing Innovation Center for Engineering Science and Advanced Technology, Peking University, Beijing 100871, China (e-mail: junzhi.yu@ia.ac.cn).

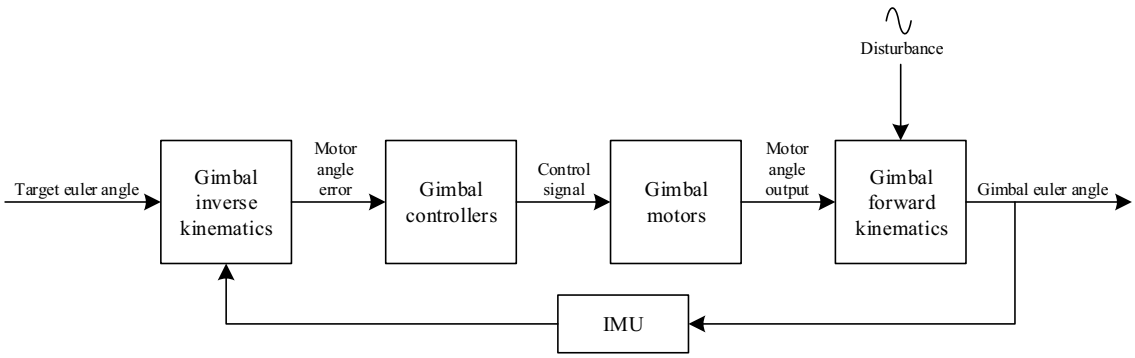

Fig. 2. System framework of 2-DOF stabilization platform (gimbal).

$$Euler(\psi,\theta,\phi)=\begin{bmatrix}\cos\psi\cos\theta & \cos\psi\sin\theta\sin\phi-\sin\psi\cos\phi & \cos\psi\sin\theta\cos\phi+\sin\psi\sin\phi\\ \sin\psi\cos\theta & \sin\psi\sin\theta\sin\phi+\cos\psi\cos\phi & \sin\psi\sin\theta\cos\phi-\cos\psi\sin\phi\\ -\sin\theta & \cos\theta\sin\phi & \cos\theta\cos\phi\end{bmatrix} \tag{5}$$

or big calculation.

Currently, there are only a few researches on camera stabilization for robotic fish. A head stability control scheme was proposed by Sun *et al.* in [13]. To minimize the swing of robotic fish's head, they built a hydrodynamics model and applied genetic algorithm to optimize joints' parameters. This method enhanced imaging stability but decreased the velocity of fish at meanwhile. In [14], Yang *et al.* developed a camera stabilizer system for robotic fish, which significantly reduced the swing of camera under the periodic disturbance from yaw channel. But there is only one DOF so that the stabilizing effect will be worse when system suffers from the disturbance of multiple directions.

This paper further tackles the problem of camera shaking for robotic fish on the basis of previous work [14]. Considering that the disturbance normally comes form yaw and roll direction when swimming, we develop a compact 2-DOF stabilization gimbal for the contained camera in robotic fish. The forward and inverse kinematics of gimbal are first derived to calculate controllers' input. Then we decouple yaw and roll channels, and control them separately using ADRC algorithm. At last, an experimental platform is designed to compare the effectiveness of various control algorithms, including PD control, feedback-feedforward control and ADRC. The results demonstrate that ADRC decreases the swing of camera to the maximum extent and achieves best stabilizing effect.

The rest of the paper is organized as follows. The problem formulation about camera stabilization is given in Section 2. The linear ADRC algorithm and parameter configuration are depicted in Section 3. In Section 4, experimental platform and corresponding results are introduced. Finally, the conclusion of this paper is presented in Section 5.

II. Problem Formulation

Acquiring stable images for environment sensing is a difficult issue especially when robotic fish swims. Aiming to tackle this issue, we develop a compact 2-DOF stabilization platform, whose objective is to reject the disturbance from fish body's swing and stabilize camera at target attitude. The figure of platform is shown in Fig. 1. This platform consists of two Hitec HS5035HD servomotors. To achieve higher response speed and control frequency, we remove the control board of servomotors as well as directly controlling DC motors.

As shown in Fig. 1, we define four frames as follows. World frame W is defined by the initial body attitude after power up, which is regarded as inertial frame in general. Fish body frame B and camera frame C are respectively aligned with the IMU frames that equipped on fish and camera. Target frame T corresponds to the desired camera attitude. Based on these definitions of frames, the problem about camera stabilization can be formulated as follow:

$$R_T^C = R_W^C \cdot R_T^W \to I \tag{1}$$

where R_T^C denotes the rotation matrix that transforms the coordinate representation of points from frame T to C, and I is identity matrix. Through controlling these two motors, we can change R_T^C to approach desired attitude.

In order to let R_T^C approximate to identity matrix, the system framework and kinematics of this 2-DOF gimbal are further analyzed. As shown in Fig. 2, the gimbal framework contains four parts. Gimbal motors have already been introduced, which are normal DC motors in servomotors. The specific structures of gimbal controllers will be discussed on subsequent section. This part mainly demonstrates the forward and inverse kinematics of 2-DOF gimbal.

Gimbal forward kinematics depict the relationship among motor rotation angle, disturbance angle and actual euler angle of camera frame, which can be modeled as follows:

$$R_C^W = R_B^W \cdot R_C^B \tag{2}$$

$$R_B^W = Rot(Z,\psi_d)\cdot Rot(Y,\theta_d)\cdot Rot(X,\phi_d) \tag{3}$$

$$R_C^B = Rot(Z,\beta_z)\cdot Rot(X,\beta_x) \tag{4}$$

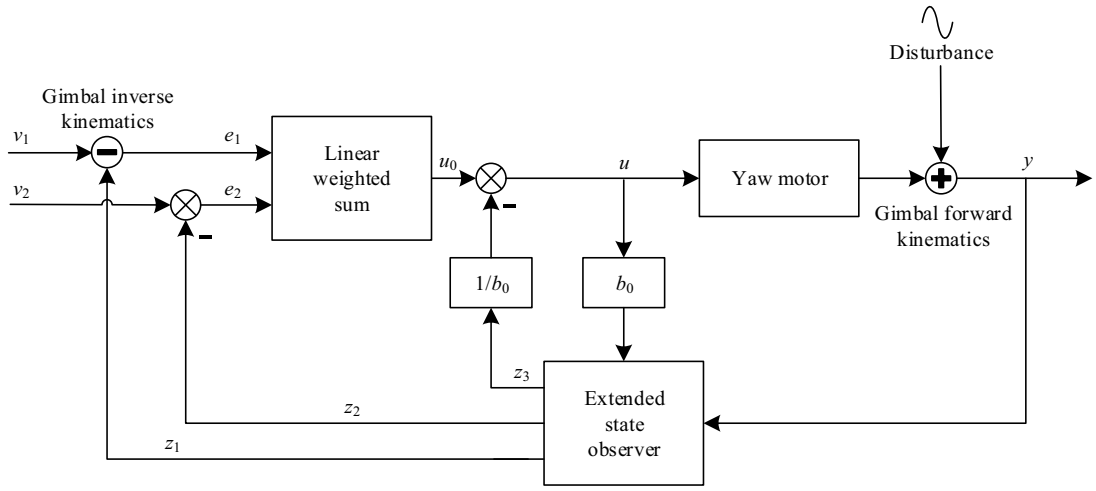

Fig. 3. Control block diagram of linear ADRC (Take yaw channel as an example).

where ψ_d, θ_d and ϕ_d separately represent the disturbance angle on yaw, pitch and roll directions, which are equal with euler angle of frame B that can be measured by the IMU mounted on fish body. β_z and β_x denote the output rotation angle of yaw motor and roll motor, respectively. Note that rotate order of euler angle used in this paper is $Z-Y-X$. The relationship between euler angle and rotation matrix is given in Eq. (5). In most cases, there is $\cos\theta > 0$, so camera euler angle ψ_c, θ_c and ϕ_c can be solved as follows according to Eq. (5).

$$\psi_c = \arctan\left[\frac{R_C^W(2,1)}{R_C^W(1,1)}\right] \tag{6}$$

$$\theta_c = \arctan\left[\frac{-R_C^W(3,1)}{R_C^W(1,1)\cdot\cos\psi_c + R_C^W(2,1)\cdot\sin\psi_c}\right] \tag{7}$$

$$\phi_c = \arctan\left[\frac{R_C^W(3,2)}{R_C^W(3,3)}\right] \tag{8}$$

In practical application, the euler angle of camera can be measured by the IMU fixed with camera. Deriving forward kinematics for gimbal is to explain the problem more clearly and later deduction.

Gimbal inverse kinematics explain how to map the differences between target and actual angle of camera into motor error angle. First, using the feedback of ψ_c, θ_c, ϕ_c, rotation matrix R_C^W can be rebuilt, and:

$$R_C^W \cdot Rot(Z,\alpha_z)\cdot Rot(X,\alpha_x) = R_T^W \tag{9}$$

then, we can get:

$$\begin{aligned} R_T^C &= R_W^C \cdot R_T^W \\ &= Rot(Z,\alpha_z)\cdot Rot(X,\alpha_x) \\ &= \begin{bmatrix} \cos\alpha_z & -\sin\alpha_z\cos\alpha_x & \sin\alpha_z\sin\alpha_x \\ \sin\alpha_z & \cos\alpha_z\cos\alpha_x & -\cos\alpha_z\sin\alpha_x \\ 0 & \sin\alpha_x & \cos\alpha_x \end{bmatrix} \end{aligned} \tag{10}$$

so,

$$\alpha_z = \arctan\left[\frac{R_T^C(2,1)}{R_T^C(1,1)}\right] \tag{11}$$

$$\alpha_x = \arctan\left[\frac{R_T^C(3,2)}{R_T^C(3,3)}\right] \tag{12}$$

where α_z and α_x denote error angle of yaw and roll motors, respectively. Note that these two angles are the input of gimbal controllers. Generally, R_T^W equals to identity matrix for most stabilization tasks. While for tracking task, R_T^W should be set with the change of target position. In this paper, stabilization task is main object, so we set $R_T^W = I$. Then α_z and α_x are further derived as:

$$\alpha_z = \arctan\left[\frac{\cos\psi_c\sin\theta_c\sin\phi_c - \sin\psi_c\cos\phi_c}{\cos\psi_c\cos\theta_c}\right] \tag{13}$$

$$\alpha_x = \arctan\left[\frac{\sin\psi_c\sin\theta_c\cos\phi_c - \cos\psi_c\sin\phi_c}{\cos\theta_c\cos\phi_c}\right] \tag{14}$$

III. Controller Design

From the view in motor controlling, yaw and roll channels are equivalent that can be controlled separately. Therefore, yaw channel will be discussed as an example in this section. In the past work [14], feedback-feedforword controller based on disturbance compensation is designed and achieves better results compared to PD controller. Inspired by the thought that compensating disturbance can enhance control effect, we find that ADRC is more appropriate for our task and not rely on extra sensors to observe disturbance.

ADRC generally consists of a tracking differentiator (TD), an extended state observer (ESO) and a nonlinear feedback combination, which references the ideas of PID controller and further overcomes its limitation [15]. Particularly, it can be designed without an explicit mathematical model of the plant. The concept and method of total disturbance estimation and rejection are significant features of it. In this paper, linear ADRC is applied in our gimbal control system, since it is easier for parameter tuning and this system is of a small nonlinearity. In camera stabilization task, input signal rarely changes, so tracking differentiator is omitted. The linear ADRC block diagram is shown in Fig. 3 and the

corresponding control algorithm is given in Eq. (15). As for Fig. 3, the input v_1 is target euler angle and v_2 is equal to zero, while e_1 is the error angle of yaw motor calculated by gimbal inverse kinematics. Furthermore, the ESO's input y can be observed through the IMU fixed on camera. For simplicity, gimbal forward and inverse kinematics can be regarded as generalized addition and substraction.

$$\begin{cases} e = z_1(k) - y(k) \\ z_1(k+1) = z_1(k) + h \cdot (z_2(k) - \beta_{01} e) \\ z_2(k+1) = z_2(k) + h \cdot (z_3(k) - \beta_{02} e + bu(k)) \\ z_3(k+1) = z_3(k) - h \cdot \beta_{03} e \\ e_1 = v_1(k) - z_1(k),\ e_2 = v_2(k) - z_2(k) \\ u_0 = k_p e_1 + k_d e_2 \\ u(k) = u_0 - z_3(k)/b \end{cases} \tag{15}$$

where h is sampling period, $\beta_{01}, \beta_{02}, \beta_{03}$ are observer gains and b is a system parameter about input gain. The control law of u reduces the plant to a double integrator, which is controlled by the PD controller. k_p and k_d are similar to the gains of the PD controller.

Particularly, based on bandwidth concept, Gao *et al.* proposed a simple method to determine parameters of linear ESO [16]. For two-order plant, the formula is as follow:

$$\beta_{01} = 3\omega_0,\ \beta_{02} = 3\omega_0^2,\ \beta_{03} = \omega_0^3 \tag{16}$$

where ω_0 denotes the bandwidth of the observer.

IV. Experimental Verification

For the sake of evaluating the effectiveness of 2-DOF gimbal, we develop an experimental platform shown in Fig. 4. Aiming to simulate the swing mode of robotic fish that controlled by central pattern generator (CPG) model [17], this platform consists of two large servomotors causing disturbance, both of which rotate as the sine wave.

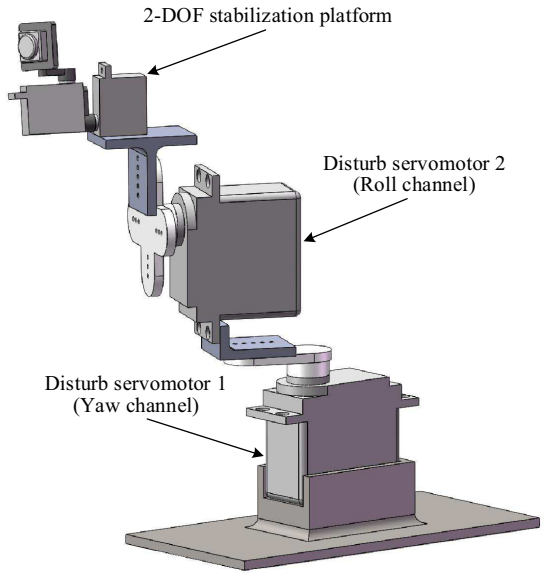

Fig. 4. The schematic diagram of the experimental platform.

TABLE I

Comparisons of amplitude responses in PD control, feedback-feedforward control and ADRC

Frequency (Hz)	Amplitude of output (°)		
	PD	FF	**ADRC**
0.25	3.20	2.56	**1.71**
0.50	4.17	2.87	**2.53**
0.75	5.79	4.37	**3.25**
1.00	7.82	6.33	**5.01**

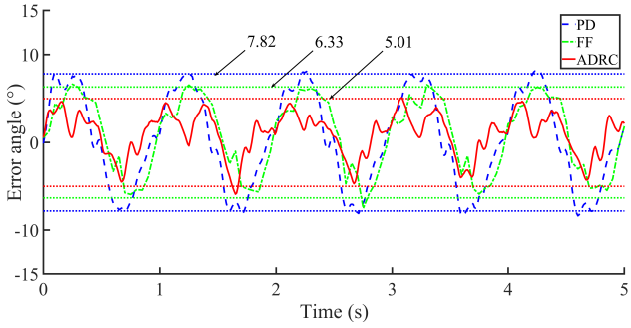

Fig. 5. Experimental results of PD control, feedback-feedforward control, and ADRC under the sine wave disturbance with frequency of 1 Hz and amplitude of 60°.

A. Control Algorithms Comparison

High-performance controller is a basic guarantee of effectiveness for the stabilization platform. In this part, ADRC is compared with traditional PD control and feedback-feedforward control proposed by [14]. Since motor controlling of both yaw and roll channels are the same, we only introduce the experimental results of one of them. Fig. 5 shows the outputs of yaw channel corresponding to three controllers under the sine wave disturbance with frequency of 1 Hz and amplitude of 60°. Compared with the other two controllers, ADRC decreases error angle from 7.82° and 6.33° to 5.01°. In addition, the detailed amplitude-frequency characteristics are listed in Table I. It can be easily found that although disturbed by motor's rotation of various frequency, the system using ADRC gets lower amplitude and more robust stabilizing effect. It might be caused by the disturbance compensation mechanism of ADRC which estimates and rejects the internal and external disturbance as total disturbance. Therefore, ADRC owns better adaptability and robustness than feedback-feedforward control that only compensates external disturbance.

B. Stabilizing Effect of Stabilization Platform

Although gimbal controllers achieve well results of disturbance rejection, the stabilizing effect of entire gimbal system are the most crucial criterion. In this part, four kinds of configurations of gimbal system are compared, including no stabilization, stabilization on yaw axes, stabilization on roll axes and stabilization on both yaw and roll axes.

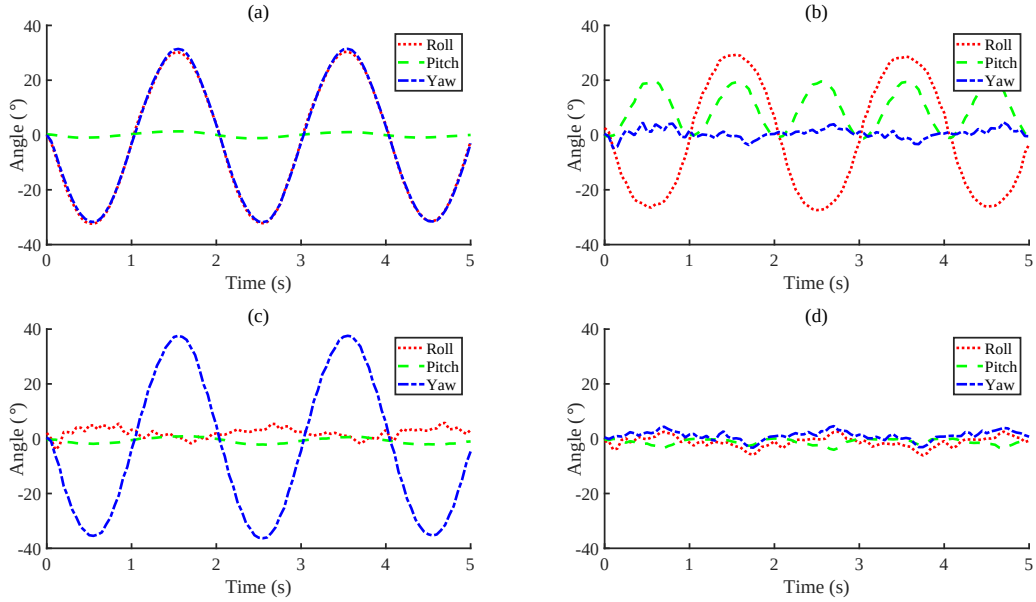

Fig. 6. Comparisons of change of euler angle in different configurations of stabilization platform. (a) No stabilization. (b) Stabilization on yaw axes. (c) Stabilization on roll axes. (d) Stabilization on both yaw and roll axes.

TABLE II

COMPARISONS OF MAXIMUM TRANSLATION OF BLACK CROSS IN DIFFERENT GIMBAL CONFIGURATIONS

Stabilization type	**Maximum translation (pixel)**			
	Left		**Right**	
	x	**y**	**x**	**y**
No stabilization	>320	>180	>320	>180
Yaw-axial stabilization	104	> 180	130	172
Roll-axial stabilization	>320	24	>320	35
Double axial stabilization	**34**	**24**	**65**	**22**

The change of camera's euler angle is first evaluated for four configurations, which can be measured by IMU fixed on camera. As shown in Fig. 6(a), no-stabilized camera entirely follows the external disturbance from yaw and roll channels, which is with 30° of amplitude and 0.5 Hz of frequency. Fig. 6(b) depicts the angle of yaw-stabilized gimbal. Although the yaw angle is stabilized at zero, extra disturbance on pitch is induced into system. In Fig. 6(c), roll-stabilized gimbal decreases the amplitude of disturbance on roll channel, but the amplitude of yaw channel is enlarged. As for Fig. 6(d), both yaw and roll channels are stabilized at the scale of 5° by 2-DOF gimbal. The experimental results demonstrate that 2-DOF gimbal performs much better than 1-DOF one, particularly when it suffers from the disturbance of two directions.

In addition, through comparing the change of camera's field of view, we evaluate the stabilizing effect of four stabilization platforms under typical disturbance. To clearly demonstrate experimental results, a cycle of pictures that correspond to four kinds of conditions are captured from the camera. The resolution of this camera is 640×360. A flat board with a black cross is placed in front of the camera and the distance is about 30 cm. We calculate the maximum translation of the center of black cross on image plane during one cycle and the results are given in Table II. A careful inspection of Table II reveals that 2-DOF gimbal limits the moving of black cross center within a range of 70 pixels, which possesses more superior performance than 1-DOF gimbal.

Finally, image sequence with four kinds of configurations are given in Fig. 7 intuitively. Fig. 7(d) shows the image sequence from camera equipped on 2-DOF stabilization platform. This stable sequence can be a direct input to most of visual algorithms as well as guaranting the robustness.

V. CONCLUSIONS AND FUTURE WORK

This paper has proposed a compact 2-DOF camera stabilization platform for acquiring stable images while robotic fish swims. First, the problem of stabilization is modeled as adjusting R_T^C to approaching to identity matrix and the specific framework of gimbal system is discussed. Then, we derive forward and inverse kinematics of gimbal and apply them on control algorithm. ADRC is employed for controlling two gimbal motors separately owing to its superior disturbance rejection ability. At last, in order to verify the effectiveness of control algorithm and stabilization platform, we develop a 2-DOF experimental platform. Experimental results demonstrate that ADRC performs better than PD and feedback-feedforward control in our application. Besides, when disturbance comes from two direction, 2-DOF stabilization platform can guarantee the stability of image but 1-DOF platform sometimes makes things worse.

The ongoing and future work will further seek for minisize actuator to reduce the size of stabilization platform and

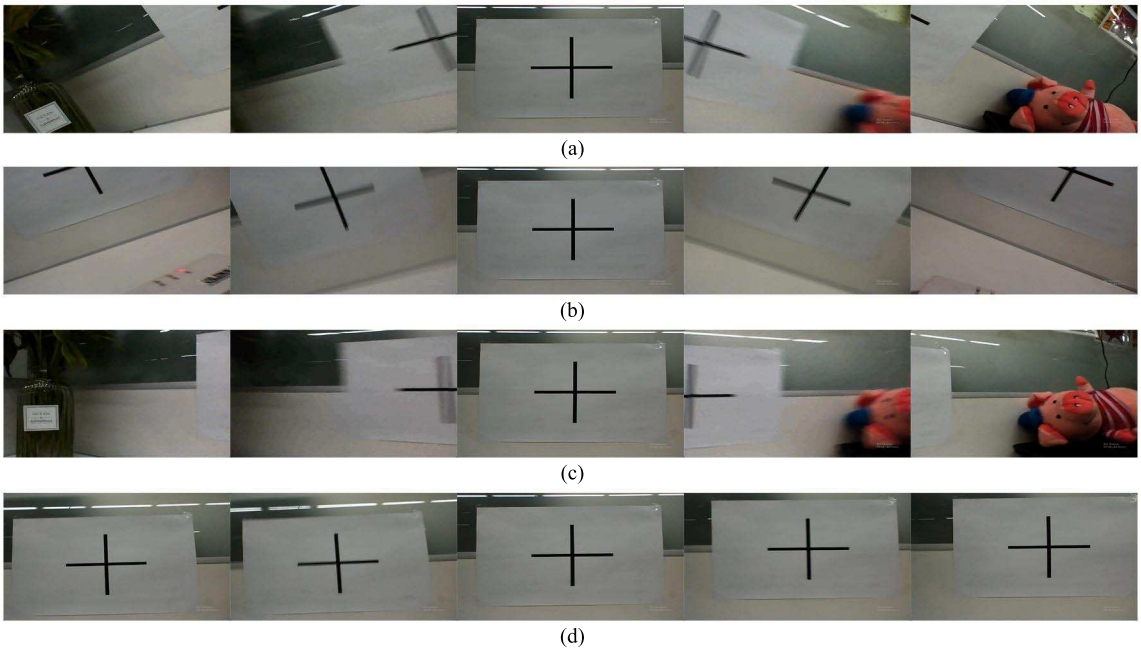

Fig. 7. Comparisons of change of field of view in different configurations of stabilization platform. (a) No stabilization. (b) Stabilization on yaw axes. (c) Stabilization on roll axes. (d) Stabilization on both yaw and roll axes.

improve control algorithm to speed up the response. In addition, benefited from 2-DOF camera stabilization platform, the vision applications for robotic fish acquire a wider scope for research space.

REFERENCES

[1] M. S. Triantafyllou and G. S. Triantafyllou, "An efficient swimming machine," *Scientific American*, vol. 272, no. 3, pp. 64–70, 1995.

[2] J. Liu and H. Hu, "Biological inspiration: From carangiform fish to multi-joint robotic fish," *Journal of Bionic Engineering*, vol. 7, no. 1, pp. 35–48, 2010.

[3] M. Conry, A. Keefe, W. Ober, M. Rufo, and D. Shane, "Bioswimmer: Enabling technology for port security," in *2013 IEEE International Conference on Technologies for Homeland Security (HST)*, Waltham, USA, pp. 364–368, 2013.

[4] J. Yu, Z. Su, M. Wang, M. Tan, and J. Zhang, "Control of yaw and pitch maneuvers of a multilink dolphin robot," *IEEE Transactions on Robotics*, vol. 28, no. 2, pp. 318–329, 2012.

[5] Z. Su, J. Yu, M. Tan, and J. Zhang, "Implementing flexible and fast turning maneuvers of a multijoint robotic fish," *IEEE/ASME Transactions on Mechatronics*, vol. 19, no. 1, pp. 329–338, 2014.

[6] Z. Wu, J. Yu, Z. Su, and T. Min, "Implementing 3-D high maneuvers with a novel biomimetic robotic fish," *IFAC Proceedings Volumes*, vol. 47, no. 3, pp. 4861–4866, 2014.

[7] F. Sun, "Embedded vision based tracking control of biomimetic robotic fish," Ph.D. dissertation, Beijing: Institute of Automation, Chinese Academy of Sciences, 2015.

[8] W. Wang and G. Xie, "Online high-precision probabilistic localization of robotic fish using visual and inertial cues," *IEEE Transactions on Industrial Electronics*, vol. 62, no. 2, pp. 1113–1124, 2015.

[9] E. Falotico, N. Cauli, K. Hashimoto, P. Kryczka, A. Takanishi, P. Dario, A. Berthoz, and C. Laschi, "Head stabilization based on a feedback error learning in a humanoid robot," in *2012 IEEE RO-MAN: The 21st IEEE International Symposium on Robot and Human Interactive Communication*, Paris, France, pp. 449–454, 2012.

[10] H. Li, J. Luo, C. Huang, Q. Huang, and S. Xie, "Design and control of 3-DOF spherical parallel mechanism robot eyes inspired by the binocular vestibule-ocular reflex," *Journal of Intelligent & Robotic Systems*, vol. 78, no. 3–4, pp. 425–441, 2015.

[11] Z. Hurák and M. Řezáč, "Combined line-of-sight inertial stabilization and visual tracking: Application to an airborne camera platform," in *Proceedings of the 48th IEEE Conference on Decision and Control (CDC) held jointly with 2009 28th Chinese Control Conference*, Shanghai, China, pp. 8458–8463, 2009.

[12] K. Hayashi, Y. Yokokohji, and T. Yoshikawa, "Tele-existence vision system with image stabilization for rescue robots," in *Proceedings of the 2005 IEEE International Conference on Robotics and Automation*, Barcelona, Spain, pp. 50–55, 2005.

[13] F. Sun, J. Yu, and D. Xu, "Stability control for the head of a biomimetic robotic fish with embedded vision," *Robot*, vol. 37, no. 2, pp. 188–195, 2015.

[14] X. Yang, Z. Wu, J. Liu, and J. Yu, "Design of a camera stabilizer system for robotic fish based on feedback-feedforward control," in *2016 35th Chinese Control Conference (CCC)*, Chengdu, China, pp. 6044–6049, 2016.

[15] J. Han, "From PID to active disturbance rejection control," *IEEE Transactions on Industrial Electronics*, vol. 56, no. 3, pp. 900–906, 2009.

[16] Z. Gao, "Scaling and bandwidth-parameterization based controller tuning," in *Proceedings of the 2003 American Control Conference*, vol. 6, Denver, USA, pp. 4989–4996, 2003.

[17] J. Yu, Z. Wu, M. Wang, and M. Tan, "CPG network optimization for a biomimetic robotic fish via PSO," *IEEE Transactions on Neural Networks & Learning Systems*, vol. 27, no. 9, pp. 1962–1968, 2016.